THE JOURNAL OF BIOLOGICAL CHEMISTRY VOL. 286, NO. 27, pp. 24046–24056, July 8, 2011

Lipoxygenases Mediate the Effect of Essential Fatty Acid in Skin Barrier Formation

A PROPOSED ROLE IN RELEASING OMEGA-HYDROXYCERAMIDE FOR CONSTRUCTION OF THE CORNEOCYTE LIPID ENVELOPE[*][S][◆]

Received for publication, April 15, 2011, and in revised form, May 9, 2011 Published, JBC Papers in Press, May 10, 2011, DOI 10.1074/jbc.M111.251496

Yuxiang Zheng[‡], Huiyong Yin[‡], William E. Boeglin[‡], Peter M. Elias[§], Debra Crumrine[§], David R. Beier[¶], and Alan R. Brash[‡1]

From the [‡]Department of Pharmacology and the Vanderbilt Institute of Chemical Biology, Vanderbilt University School of Medicine, Nashville, Tennessee 37232, the [§]Department of Dermatology, University of California, San Francisco, San Francisco, California 94122, and the [¶]Division of Genetics, Department of Medicine, Brigham and Women's Hospital, Harvard Medical School, Boston, Massachusetts 02115

A barrier to water loss is vital to maintaining life on dry land. Formation of the mammalian skin barrier requires both the essential fatty acid linoleate and the two lipoxygenases 12*R*-lipoxygenase (12*R*-LOX) and epidermal lipoxygenase-3 (eLOX3), although their roles are poorly understood. Linoleate occurs in *O*-linoleoyl-*ω*-hydroxyceramide, which, after hydrolysis of the linoleate moiety, is covalently attached to protein via the free *ω*-hydroxyl of the ceramide, forming the corneocyte lipid envelope, a scaffold between lipid and protein that helps seal the barrier. Here we show using HPLC-UV, LC-MS, GC-MS, and ^{1}H NMR that *O*-linoleoyl-*ω*-hydroxyceramide is oxygenated in a regio- and stereospecific fashion by the consecutive actions of 12*R*-LOX and eLOX3 and that these products occur naturally in pig and mouse epidermis. 12*R*-LOX forms 9*R*-hydroperoxy-linoleoyl-*ω*-hydroxyceramide, further converted by eLOX3 to specific epoxyalcohol (9*R*,10*R*-*trans*-epoxy-11*E*-13*R*-hydroxy) and 9-keto-10*E*,12*Z* esters of the ceramide; an epoxy-ketone derivative (9*R*,10*R*-*trans*-epoxy-11*E*-13-keto) is the most prominent oxidized ceramide in mouse skin. These products are absent in 12*R*-LOX-deficient mice, which crucially display a near total absence of protein-bound *ω*-hydroxyceramides and of the corneocyte lipid envelope and die shortly after birth from transepidermal water loss. We conclude that oxygenation of *O*-linoleoyl-*ω*-hydroxyceramide is required to facilitate the ester hydrolysis and allow bonding of the *ω*-hydroxyceramide to protein, providing a coherent explanation for the roles of multiple components in epidermal barrier function. Our study uncovers a hitherto unknown biochemical pathway in which the enzymic oxygenation of ceramides is involved in building a crucial structure of the epidermal barrier.

In 1929, Burr and Burr (1) famously reported the existence of essential fatty acids (EFA)[2] and noted the most obvious symptom of EFA deficiency as "an abnormal, scaly condition of the skin." This phenotype is associated with accelerated transepidermal water loss that reflects defects in water barrier function (2) and thus resembles the human genetic disorders of ichthyosis, diseases with a dry, thickened, scaly skin (3, 4). Linoleate (C18:2) is by far the most abundant EFA in the epidermis, being mainly esterified to the *ω*-hydroxyl of the amide-linked very long chain fatty acid (VLFA) in a unique class of ceramides, namely esterified omega-hydroxyacyl-sphingosine (EOS) (5). A portion of EOS is further converted to omega-hydroxyacyl-sphingosine (OS) and *ω*-hydroxy-VLFA that are covalently attached to the external face of the cornified cell envelope (CE) composed of cross-linked proteins (Fig. 1) (6–9). These covalently bound lipids are the main component of the corneocyte lipid envelope (CLE) (10), which, together with the underlying CE, constitutes a structure indispensable to the integrity of the epidermal water barrier (5, 11).

EFA contain at least two CH_2-interrupted *cis* double bonds, and as such they are potential substrates for oxygenation by lipoxygenase (LOX) enzymes. In fact, there are two epidermis-specific lipoxygenases, ALOX12B and ALOXE3, that, if mutated to inactive forms, cause a barrier-related disease, autosomal recessive congenital ichthyosis (4, 12). Mouse knock-out models confirm a severely defective barrier phenotype (13–15). Because the same symptoms are caused by mutation of either gene, the encoded proteins 12*R*-lipoxygenase (12*R*-LOX) and epidermal lipoxygenase-3 (eLOX3) are proposed to function in the same pathway of skin barrier formation (12, 16). Biochemical studies also suggest that the two enzymes act in tandem: 12*R*-LOX first makes a specific hydroperoxide from a fatty acid substrate, and eLOX3 in turn converts the 12*R*-LOX product

* This work was supported, in whole or in part, by National Institutes of Health Grants AR051968 (to A. R. B.), AR019098 (to P. M. E.), and HD36404 (to D. R. B.).

◆ This article was selected as a Paper of the Week.

[S] The on-line version of this article (available at http://www.jbc.org) contains supplemental Table S1 and Figs. S1–S6.

[1] To whom correspondence should be addressed: Dept. of Pharmacology, Vanderbilt University, Nashville, TN 37232-6602. Tel.: 615-343-4495; Fax: 615-322-4707; E-mail: alan.brash@vanderbilt.edu.

[2] The abbreviations used are: EFA, essential fatty acid(s); LOX, lipoxygenase; eLOX3, epidermal lipoxygenase-3; HODE, hydroxy-octadecadienoic acid; HPODE, hydroperoxy-octadecadienoic acid; KODE, keto-octadecadienoic acid; EpOH, epoxyalcohol; EOS, esterified omega-hydroxyacyl-sphingosine; OS, omega-hydroxyacyl-sphingosine; Glc-EOS, acylglucosylceramides; RP, reversed phase; APCI-MS, atmospheric pressure chemical ionization; VLFA, very long chain fatty acid(s); CE, corneocyte envelope; CLE, corneocyte lipid envelope; CHAPS, 3-[(3-cholamidopropyl)dimethylammonio]-1-propanesulfonic acid.

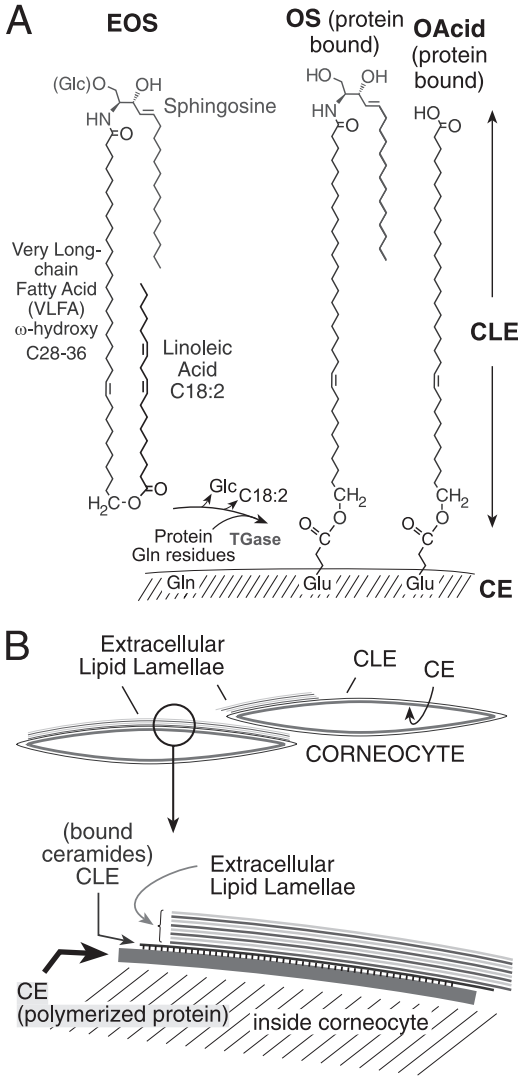

FIGURE 1. **Esterified ceramides of the mammalian epidermal barrier.** *A*, EOS in the outer epidermis is esterified mainly with linoleic acid (C18:2) and is glucosylated at C-1 of the sphingosine (Glc-EOS) early in differentiation. After hydrolysis of the glycosidic and ester bonds, the resulting OS is esterified by transglutaminase (*TGase*) to glutamines in the cross-linked proteins of the CE (9). The ester linkage in the resulting glutamates bonds the monomolecular lipid coating, the CLE, to the outer face of the CE. ω-Hydroxy-VLFA (OAcid, shown on the *right side*) are also ester-linked components of the CLE. *B*, the CE is a highly cross-linked protein coat at the cell periphery, bonded with the extracellular lipid milieu via the CLE, with a detailed view illustrated in the segment below.

into a specific epoxyalcohol (16). However, the physiological substrate of 12*R*-LOX and eLOX3 in the epidermis and the specific function of the LOX products in skin barrier formation remain to be identified.

Two further observations lead us to propose a model that can explain simultaneously the roles of 12*R*-LOX, eLOX3, and EFA in the mammalian epidermis. In essential fatty acid deficiency, in which linoleate in the EOS ceramides is replaced by oleate (not a lipoxygenase substrate) (17), the protein-bound ω-hydroxyceramides are significantly decreased (18). Similarly, there is evidence that in the 12*R*-LOX$^{-/-}$ mouse epidermis, the protein-bound ω-hydroxyceramides are also decreased (14). Although LOX enzymes typically act on free fatty acids (and indeed 12*R*-LOX gets its name from its reaction with arachidonic acid), we hypothesized that the two LOX enzymes oxygenate the linoleate esterified in EOS and that this LOX-catalyzed oxygenation is required to facilitate hydrolysis of the (oxidized) linoleate moiety, exposing the ω-hydroxyl of the VLFA moiety for coupling to the CE proteins and thus forming the CLE. To test this hypothesis, we examined the proposed reactions using recombinant human LOX enzymes and analyzed lipid extracts from pig and mouse epidermis for the presence of naturally occurring oxidized ceramides. With the aid of a 12*R*-LOX$^{-/-}$ mouse model, we evaluated the impact of the putative 12*R*-LOX-eLOX3 pathway on the profiles of both free and covalently bound ceramides and on the CLE structure in the stratum corneum of mouse epidermis.

EXPERIMENTAL PROCEDURES

Materials

HODE methyl ester standards were synthesized by autoxidation of methyl linoleate (NuChek Prep Inc.) followed by triphenylphosphine reduction and HPLC purification. HODE free acid standards were generated by alkaline hydrolysis of the corresponding methyl esters or by reacting soybean LOX-1 (Sigma-Aldrich) or *Anabaena* LOX (19) with linoleic acid (NuChek Prep Inc.). The generation of 12*R*-LOX-deficient mice via *N*-ethyl-*N*-nitrosourea mutagenesis and methods for their identification by genotype analysis have been described previously (13). Human 12*R*-LOX and human eLOX3 were expressed and purified as described previously (20).

Preparation of Epidermis

Sections of pig skin (~10 cm × 10 cm) were immersed in 65 °C water for 2 min, and then the epidermis was separated from the dermis using a razor blade. Mouse epidermis was isolated after treating the skin with 1.5 mg/ml Dispase II (Roche Applied Science) in phosphate-buffered saline at 4 °C overnight.

Lipid Extraction

The epidermis was homogenized in chloroform-methanol mixtures (1:1 and 2:1, v/v). The organic layer was separated from the protein pellet by centrifugation. This was repeated four times. The lipids were extracted by the Bligh and Dyer method (21). The lipid extract was dried using a rotary evaporator or under a stream of N_2 and then redissolved in chloroform-hexane (1:1, v/v). The lipid extract was then loaded onto a pre-equilibrated solid phase silica column (Bond Elut, Varian, Inc.), washed with chloroform-hexane (1:1, v/v), and eluted with chloroform and chloroform-methanol (2:1, v/v).

Isolation of Glc-EOS and EOS from Pig Epidermis

Glc-EOS and EOS were isolated from the lipid extract by normal phase HPLC with APCI-MS detection (22). Normal phase HPLC used a Waters 2695 pump, a Beckman Silica Ultrasphere column (5 μm, 1 × 25 cm), a gradient program from chloroform to chloroform-isopropanol (1:1, v/v) in 15 min, and a flow rate of 5 ml/min. An Upchurch Scientific TEE was used to split the flow between the fraction collector and the mass spectrometer, a Finnigan LCQ deca XP, or a Finnigan LTQ

instrument (Thermo Electron). The APCI vaporizer temperature was set to 500 °C, and the capillary temperature was set to 150 °C. The spectra were obtained in full scan mode monitoring positive ions between *m*/*z* 400 and *m*/*z* 1500.

Reactions of 12R-LOX and eLOX3 with Glc-EOS or EOS in Vitro

Isolated Glc-EOS (final concentration, 60 μM) or EOS (final concentration, 40 μM), together with the antioxidant 4-hydroxy-TEMPO (4-hydroxy-2,2,6,6-tetramethylpiperidin-1-oxyl; final concentration, 1 mM; Sigma-Aldrich) (23), was taken to dryness under a stream of N_2. The lipids were dispersed in 2 ml of sodium phosphate, pH 6.0, with 10 mM CHAPS (Sigma-Aldrich) by sonication on ice and then incubated with 12*R*-LOX (final concentration, 5 μM) at room temperature for 2 h. To study the reaction of eLOX3, HPLC-purified 12*R*-LOX products (final concentration, 10–15 μM) were dispersed in 1 ml of sodium phosphate, pH 7.5, with 10 mM CHAPS by sonication on ice and then incubated with eLOX3 (final concentration, 5 μM) at room temperature for 2 h. Both 12*R*-LOX and eLOX3 products were extracted by the Bligh and Dyer method (21).

HPLC-UV and LC-MS Analysis of the 12R-LOX and eLOX3 Reactions with Glc-EOS

All of the HPLC-UV analyses used an Agilent 1100 or 1200 system with diode array detection. The reactions with Glc-EOS were analyzed by RP-HPLC-UV analysis using a Zorbax Eclipse XDB-C8 column (5 μm, 4.6 μm × 15 cm), an isocratic solvent system of methanol/hexane (10:1, v/v) for 12*R*-LOX reaction or methanol/water (100:2, v/v) for eLOX3 reaction, and a flow rate of 1 ml/min. The reactions with EOS were analyzed by normal phase HPLC-UV analysis using a Beckman Silica Ultrasphere column (5 μm, 4.6 mm × 25 cm), a solvent system of hexane/isopropanol/acetic acid (90:10:0.1, v/v/v), and a flow rate of 1 ml/min. Prior to LC-MS analysis, 12*R*-LOX products were reduced with excess triphenylphosphine, because hydroperoxides were not stable under the used APCI conditions. LC-MS analysis used the same chromatography conditions as the corresponding HPLC-UV analysis and the same APCI-MS conditions as described under "Isolation of Glc-EOS and EOS from Pig Epidermis."

Recovery of Ester-linked Protein-bound Lipids

After removal of free and reversibly bound lipids, protein pellets were incubated in 1 M KOH in 95% methanol at room temperature overnight. The methanolic layer was removed after centrifugation, neutralized with 1 N HCl, and then extracted by the Bligh and Dyer method (21). The protein pellet was washed by chloroform-methanol (1:1, v/v), which was then extracted by the Bligh and Dyer method. The organic phases were combined, dried, and redissolved in the LC solvent.

HPLC-UV and LC-MS Analysis of Naturally Occurring Epidermal Ceramides

All HPLC-UV analysis was performed on an Agilent 1100 or 1200 system with diode array detection. NP-HPLC-UV analysis used a Beckman Silica Ultrasphere column (5 μm, 4.6 mm × 25 cm), a solvent system of hexane/isopropanol/acetic acid (90:10:0.1, v/v/v), and a flow rate of 1 ml/min. After the analysis, polar lipids retained on the column were eluted with hexane/isopropanol/acetic acid (50:50:0.1, v/v/v) at a flow rate of 1 ml/min. The same chromatography conditions were used for LC-MS analysis. For analysis of free and reversibly protein-bound ceramides, the APCI vaporizer temperature was set to 500 °C, and the capillary temperature was set to 150 °C. For analysis of ester-linked protein-bound ω-hydroxyceramides, the APCI vaporizer temperature was set to 275 °C, and the capillary temperature was set to 250 °C. The spectra were obtained in full scan mode monitoring positive ions.

Transesterification of Oxygenated Ceramides and HPLC-UV and GC-MS Analysis of the Methyl Esters

HPLC-purified samples were incubated with 0.16 M sodium methoxide in chloroform-methanol (2:1, v/v) at room temperature for 1 h. After the reaction, the mixture was acidified by 1 M KH_2PO_4, and the organic phase was washed twice with water before being dried and redissolved in the HPLC solvent. Normal phase HPLC-UV analysis of HODE methyl esters used a Beckman Silica Ultrasphere column (5 μm, 4.6 mm × 25 cm), a solvent system of hexane/isopropanol (100:1.5 or 100:2, v/v), and a flow rate of 1 ml/min. Chiral HPLC-UV analysis of HODE methyl esters used a solvent system of hexane/methanol/ethanol (100:5:5, v/v/v), with either a Chiralpak AD column (5 μm, 4.6 mm × 25 cm) eluted at 1 ml/min, or a Chiralpak AD-H column (5 μm, 2.1 mm × 15 cm) eluted at 0.2 ml/min. Normal phase HPLC-UV analysis of epoxyalcohol methyl esters used a Beckman Silica Ultrasphere column (5 μm, 4.6 mm × 25 cm), a solvent system of hexane/isopropanol (100:2 or 100:1.5, v/v), and a flow rate of 1 ml/min. GC-MS analysis of epoxyalcohol methyl esters was performed as described previously (24).

Preparation, Identification, Assignment of Chirality, and Absolute Configuration of the 9,10-Epoxy-11E-13-hydroxy-octadecenoate Epoxyalcohols

Preparation of 9S-HPODE and Racemic 9-HPODE—9*S*-HPODE was prepared from linoleic acid using an extract of potato tuber (containing 9*S*-LOX) (25). Racemic 9-HPODE methyl ester was prepared by vitamin E-controlled autoxidation of methyl linoleate as described (26). The hydroperoxides were purified by normal phase HPLC.

Preparation of Epoxyalcohols—Epoxyalcohols were generated by reacting 9*S*-HPODE or racemic 9-HPODE with hematin as described previously (27). A group of four isomeric 9,10-epoxy-10*E*-13-hydroxy epoxyalcohols was resolved by normal phase HPLC using an Ultrasphere silica column, 5μ, 25 × 0.46 cm, with a solvent hexane/isopropanol/glacial acetic acid (100:2:0.02, v/v/v) at 1 ml/min. These products were converted to the methyl ester derivatives using diazomethane and repurified by normal phase HPLC using the solvent of hexane/isopropanol 100:2 (v/v) at a flow rate of 1 min/min with UV detection at 205 nm.

^{1}H NMR—The proton NMR spectrum and COSY of each of the four main epoxyalcohol methyl esters purified from the hematin reaction was recorded in C_6D_6, allowing their characterization as four isomers of 9,10-epoxy-11*E*-13-hydroxy-octadecenoates, a more abundant pair of *trans*-epoxides

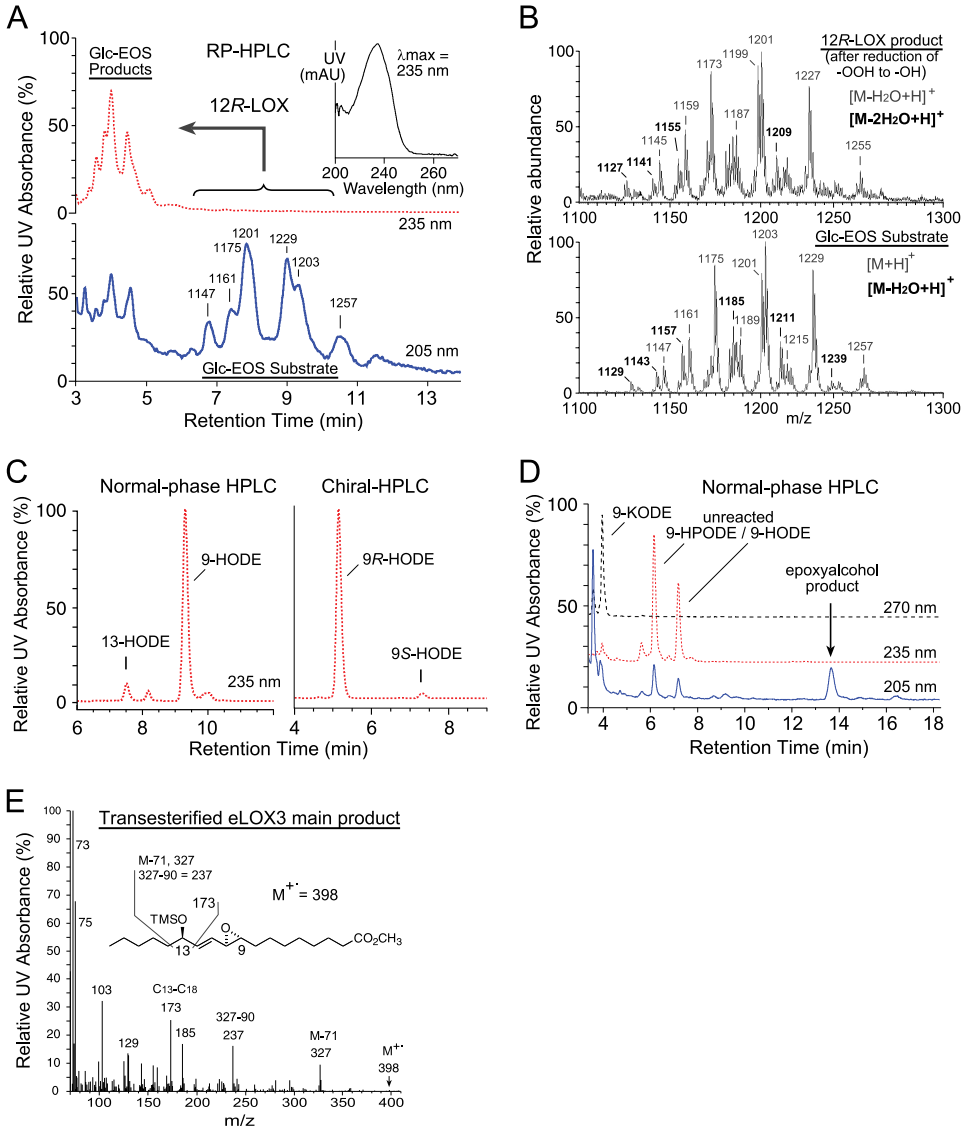

FIGURE 2. **Transformation of Glc-EOS by 12*R*-LOX and eLOX3 *in vitro*.** *A*, RP-HPLC analysis of the oxygenation of Glc-EOS by 12*R*-LOX. The Glc-EOS substrates containing esterified linoleate (and differing in chain length and number of double bonds of the amide linked fatty acid) elute at ~6.5–11 min and are detected by UV recording at 205 nm (*lower trace*, *blue*) and by APCI-MS of the $[M+H]^+$ ions at the *m/z* values indicated. The oxygenated products elute at ~3.5–5 min and are detected at 235 nm (*upper trace*, *red*). *Inset*, UV spectrum of the products. *B*, combined mass spectra of the substrates (*lower panel*) and products (*upper panel*). *C*, normal phase HPLC analysis (*left panel*) and chiral HPLC (*right panel*) of the reduced and transesterified 12*R*-LOX products as methyl esters. *D*, analysis of the reaction of eLOX3 with the 9*R*-hydroperoxides of Glc-EOS. Normal phase HPLC of the transesterified products reveals a keto derivative at 4 min of retention time (detected at 270 nm) and the major epoxyalcohol product eluting at 13.6 min (detected at 205 nm); the epoxyalcohol was identified by co-chromatography with authentic standard on HPLC (*cf.* Fig. 3*C*) and by GC-MS of the methyl ester trimethylsilyl ether derivative (*E*). *E*, GC-MS analysis of the main epoxyalcohol product from the reaction of eLOX3 with 9*R*-HPODE-Glc-EOS. Prior to the analysis, the product was transesterified to the methyl ester and derivatized to the TMS ether.

($J_{9,10}$ = 2 Hz), and a more minor pair of *cis* epoxides ($J_{9,10}$ = 4.3 Hz).

CD Spectroscopy—A 25-μg aliquot of the methyl esters of each of the two *trans*-epoxy epoxyalcohol diastereomers was converted to the 13-benzoate ester by reaction with benzoyl chloride as described (16). The CD spectrum of each purified diastereomer was then recorded using a Jasco J-700 spectropolarimeter. The diastereomer methyl ester that eluted first on normal phase HPLC gave a CD spectrum with a positive Cotton effect at 225 nm. The second eluting diastereomer gave the mirror image spectrum (negative Cotton effect). Based on the principles expounded in the original method (28) and applied to epoxyalcohols (16) and knowing the configuration at C-9 is 9*S* and that the epoxide is 9,10-*trans* (and therefore 9*S*,10*S*), the first eluting diastereomer on HPLC can be assigned as 9*S*,10*S*,13*S* and the second as 9*S*,10*S*,13*R*. The natural product from epidermis and the product of 12*R*-LOX/eLOX3 is the enantiomer of the first eluting peak from the silica column, *i.e.* of the 9*R*,10*R*,13*R* configuration.

Chiral HPLC Analysis to Determine the Absolute Configuration of Epoxyalcohols—Chiral HPLC analysis was conducted on the epoxyalcohol methyl esters using a Chiralpak AD-H column (15 × 0.2 cm; Chiral Technologies, Exton, PA) with a solvent of hexane/EtOH/MeOH (100:5:5, v/v/v), a flow rate of 0.3 ml/min, with UV detection at 205 nm. The enantiomers eluted at 21.5 min (9*R*,10*R*,13*R*) and 26 min (9*S*,10*S*,13*S*). The

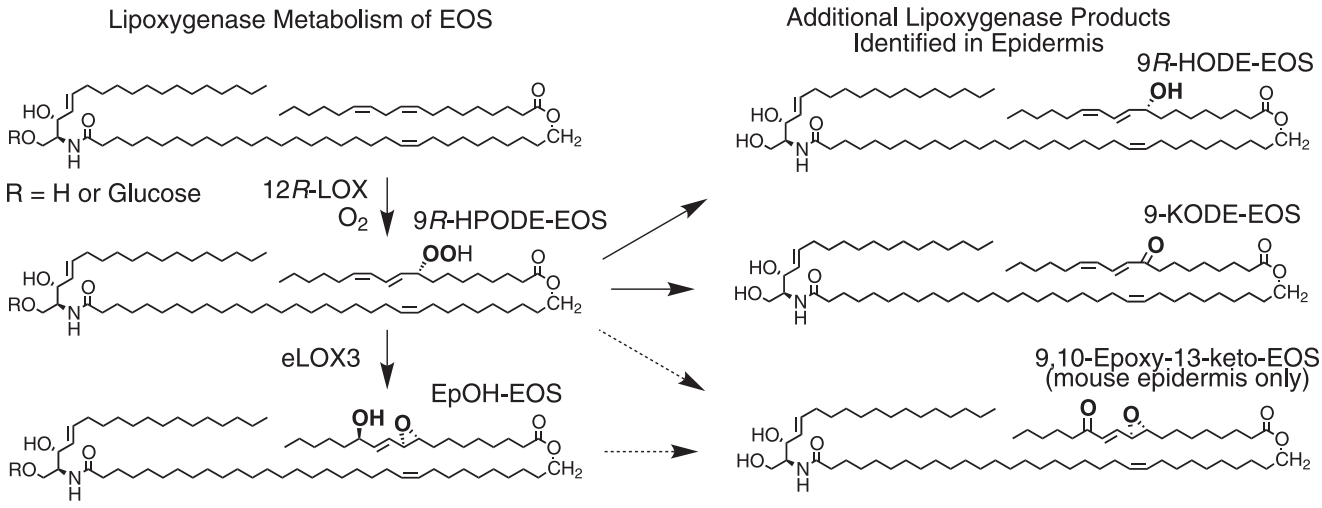

SCHEME 1

absolute configuration was established using the 9*S*,10*S*,13*S* standard prepared from 9*S*-HPODE; it eluted as the second peak from the chiral column, indicating that the first eluting enantiomer has the 9*R*,10*R*,13*R* configuration.

LC-MS Analysis of ω-Hydroxy VLFA and Epoxy-ketone Acyl Acid

RP-HPLC used a Waters Symmetry C18 column (5 mm, 2.1 mm × 15 cm), an isocratic solvent system of methanol/acetic acid (100:0.01 v/v) for ω-hydroxy VLFA or methanol/hexane/acetic acid (100:10:0.01, v/v/v) for epoxy-ketone acyl acid, and a flow rate of 0.2 ml/min. Electrospray ionization-MS used a Thermo Finnigan LTQ instrument. Mass spectra were acquired over the mass range *m*/*z* 200–1000 at 2 s/scan under the negative ion mode.

Electron Microscopy

Mouse skin samples, ~1 mm^2, were cut from frozen tissue and prefixed with Karnovsky's fixative, either before or after immersion in absolute pyridine for 2 h, a lipid extraction technique that enhances visualization of the CLE (29). The samples were postfixed in either 1% OsO_4 in 0.1 M cacodylate buffer, pH 7.3, or in RuO_4. Ultrathin sections were examined in a Zeiss 10A electron microscope.

RESULTS

Lipoxygenase Metabolism of EOS in Vitro—To test whether 12*R*-LOX and eLOX3 react with the acyl(glucosyl)ceramides *in vitro*, first we isolated and characterized the acylglucosylceramides, Glc-EOS, from pig epidermis. In agreement with previous studies of others (30, 31), the isolated Glc-EOS were a group of structural analogues varying in chain length and number of double bounds of the amide-linked VLFA and the sphingosine base, the major species of which were detected by RP-HPLC-APCI-MS as *m*/*z* 1175, *m*/*z* 1201, *m*/*z* 1203, and *m*/*z* 1229 (Fig. 2, *A* and *B*). The identity of these compounds as Glc-EOS was further confirmed by in-source fragmentation during the APCI-MS analysis, giving rise to acylceramides (EOS) with a loss of glucose.

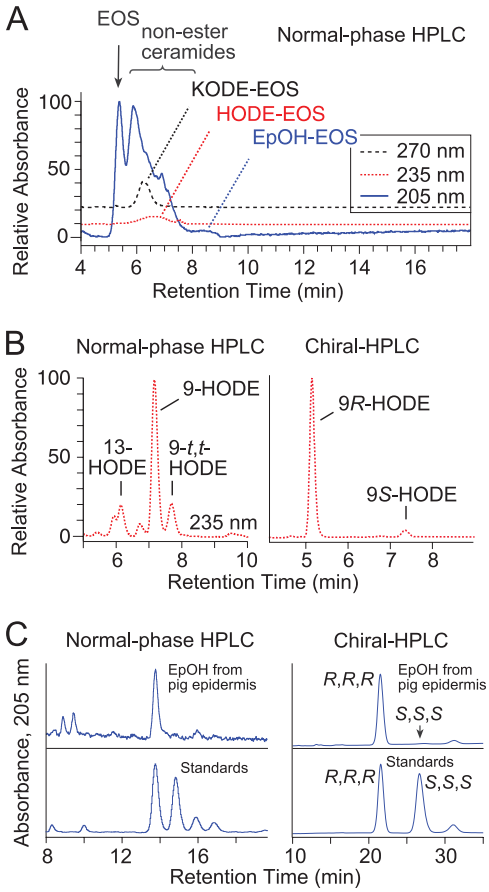

FIGURE 3. **Identification of oxygenated EOS ceramides in pig epidermis.** *A*, normal phase HPLC with UV detection reveals KODE-EOS (270 nm, *black trace*), containing a keto derivative of linoleate, HODE-EOS (235 nm, *red trace*) containing hydroxy-linoleate, and EpOH-EOS (205 nm, *blue trace*) containing an epoxyalcohol derivative of linoleate. Unmodified EOS and other known ceramides are also detected at 205 nm (5–7 min). *B*, following transesterification, the main hydroxy product is identified as 9-HODE, and chiral HPLC reveals that it is predominantly 9*R*-HODE. *C*, transesterified EpOH-EOS shows a single peak (*top panels*), corresponding to a standard of 9,10-*trans*-epoxy-13-hydroxy-octadeca-11*E*-enoate methyl ester (details in SI Methods). Chiral HPLC analysis of the natural diastereomer (*top panels*) shows that it corresponds exclusively to the 9*R*,10*R*,13*R* enantiomer of a racemic standard (*bottom panels*).

TABLE 1
APCI-mass spectrometry of EOS and EpOH-EOS

EOS				EpOH-EOS			
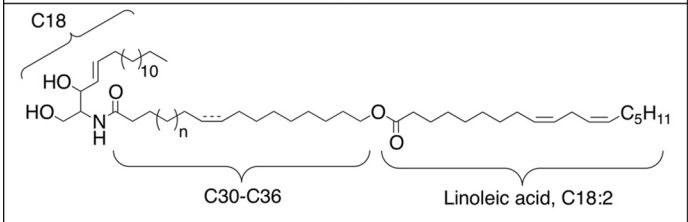				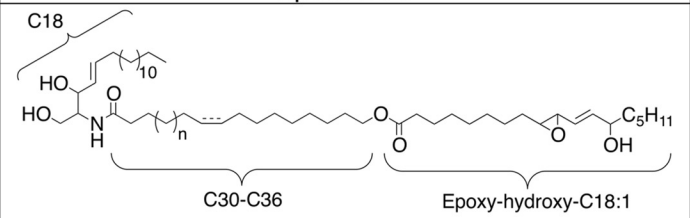			
N-acyl VLFA	Ester-linked fatty acid	$[M+H]^+$ (abundance)	$[M–H_2O+H]^+$ (abundance)	N-acyl VLFA	Ester-linked fatty acid	$[M+H]^+$ (abundance)	$[M–H_2O+H]^+$ (abundance)
C30:0	Linoleic acid	1013 (33)	995 (44)	C30:0	EpOH-C18:1	1045 (32)	1027(38)
C32:1	Linoleic acid	1039 (34)	1021 (48)	C32:1	EpOH-C18:1	1071 (47)	1053 (50)
C32:0	Linoleic acid	1041 (78)	1023 (100)	C32:0	EpOH-C18:1	1073 (67)	1055 (93)
C34:1	Linoleic acid	1067 (63)	1049 (93)	C34:1	EpOH-C18:1	1099 (65)	1081 (100)
C34:0	Linoleic acid	1069 (69)	1051 (90)	C34:0	EpOH-C18:1	1101 (54)	1083 (75)
C36:1	Linoleic acid	1095 (41)	1077 (72)	C36:1	EpOH-C18:1	1127 (30)	1109 (41)

Recombinant 12*R*-LOX reacted with either Glc-EOS (or EOS, shown in supplemental Fig. S1) to give a group of more polar Glc-EOS derivatives with absorbance at 235 nm, each displaying the characteristic UV spectrum of a conjugated diene, as expected from LOX-catalyzed oxygenation of the linoleate to a hydroperoxide, with conjugation of the double bonds (Fig. 2*A*). The product peaks were pooled, reduced to the hydroxy derivative, transesterified to the methyl ester, and subsequently analyzed by HPLC including chiral HPLC in comparison to authentic standards. 9-Hydroxy-octadecadienoate (9-HODE) was identified as the predominant product, and it was almost exclusively of the 9*R* chirality (Fig. 2*C*).

Next, we incubated 9*R*-HPODE-Glc-EOS (the hydroperoxide produced by 12*R*-LOX) with eLOX3. RP-HPLC-APCI-MS analysis identified a group of products with retention times shorter than those of the 9*R*-HPODE-Glc-EOS substrate and molecular masses 32 atomic mass units (*i.e.* the mass of two oxygen atoms) higher than Glc-EOS. When transesterified into the methyl esters, these compounds gave rise to a single epoxyalcohol (EpOH) methyl ester as the major product, which was identified by normal phase HPLC and GC-MS analysis in comparison with authentic standards (and assuming the 9*R* configuration is retained) as methyl 9*R*,10*R*-*trans*-epoxy-13*R*-hydroxy-octadeca-11*E*-enoate (Fig. 2, *D* and *E*; and supplemental Table S1 gives the ^{1}H-NMR data of this epoxyalcohol formed by eLOX3 from 9*R*-HPODE methyl ester). A minor keto product (Fig. 1*D*) was identified as 9-keto-octadecadienoate (9-KODE; Fig. 2*D*).

Nonglycosylated 9*R*-HPODE-EOS reacted similarly with eLOX3 (supplemental Fig. S1). Together, these results identify a pathway in which 12*R*-LOX and eLOX3 can act in tandem on the linoleate moiety of Glc-EOS or EOS to generate specific derivatives of 9*R*-hydroperoxy-linoleoyl-Glc-EOS with remarkable regio- and stereospecificity (Scheme 1).

Transformation of Glc-EOS or EOS by 12*R*-LOX and eLOX3 *in vitro* was exceptionally slow compared with typical LOX reactions (*e.g.* 5 μM 12*R*-LOX catalyzed only ~20% conversion of 40 μM EOS to product in 2 h). We attribute this slow reaction to the very marked insolubility of the EOS esters in aqueous solution. In our best attempts, we found that micromolar concentrations of Glc-EOS or EOS could be partially dissolved upon sonication in aqueous buffers, pH 5–7, in the presence of 10 mM CHAPS. Nonetheless, regiospecific and chiral products are formed, indicating that the transformation proceeds under tight enzymatic control.

LOX Metabolites of EOS in Pig Epidermis—Having observed the reaction of 12*R*-LOX and eLOX3 with the acylceramides *in vitro*, we searched for their metabolites *in vivo*, initially in pig epidermis. Because the LOX metabolites could be present in relatively small amounts, we developed a sensitive method for ceramide analysis using isocratic normal phase HPLC elution followed by either diode array or APCI-MS detection. With normal phase HPLC, we detected three groups of novel ceramides in pig epidermis with HPLC mobility and UV absorption consistent with LOX metabolites of EOS (Fig. 3*A*). LC-MS analysis indicated that these three groups of EOS derivatives were, in order of elution, KODE-EOS, HODE-EOS, and EpOH-EOS. For example, the molecular masses of EpOH-EOS were heavier than those of EOS by 32 atomic mass units, corresponding to the two incorporated oxygen atoms in EpOH-EOS (Table 1 and supplemental Fig. S2*A*). The ceramide structures are difficult to interpret from mass spectral data alone, because the presence of different chain length amide-linked VLFA components in EOS gives rise to a complex array of ions. Accordingly, our

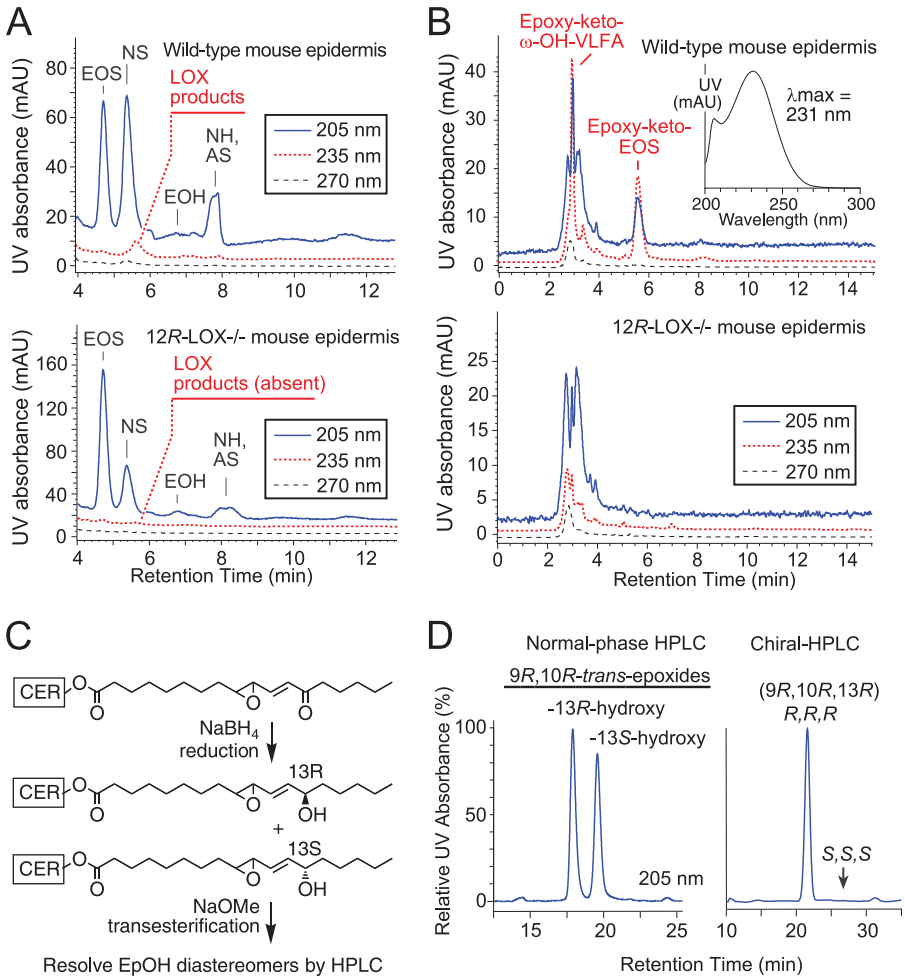

FIGURE 4. **Oxygenated EOS ceramides of mouse epidermis; absence in 12*R*-LOX$^{-/-}$ mice.** *A*, normal phase HPLC of the ceramides extracted from wild-type (*top panel*) and 12*R*-LOX-deficient mouse epidermis (*bottom panel*). Ceramides identified by MS include EOS, non-hydroxy-fatty acid sphingosine (*NS*), α-hydroxy-fatty acid sphingosine (*AS*), and non-hydroxy-fatty acid hydroxysphingosine (*NH*). *B*, normal phase HPLC of mouse epidermal lipids recovered from a final soak for 24 h at room temperature after exhaustive chloroform-methanol extractions at 0 °C, from wild-type epidermis (*top panel*) and 12*R*-LOX$^{-/-}$ (*bottom panel*). *Top panel, inset*, typical UV spectrum of products I and II in normal phase HPLC solvent. *C*, because of its instability during transesterification, the epoxy-ketone derivative in the ceramides was first reduced using $NaBH_4$ and then analyzed as the resulting epoxyalcohol diastereomers. *D*, normal phase HPLC separation of the $NaBH_4$ reduction products. Chiral HPLC analysis shows that the first eluting diastereomer is 9*R*,10*R*-epoxy-11*E*-13*R*-hydroxy-octadecenoate, identical to the epoxyalcohol product of 12*R*-LOX and eLOX3 observed in pig epidermis and *in vitro* (*cf.* Fig. 2*D* and supplemental Fig. S2).

structural analysis, although supported by the LC-MS data on the intact, oxidized ceramides, is also founded on the UV spectral characteristics of the oxidation products (conjugated diene, enone, or dieone) and on HPLC-UV and GC-MS analysis by comparison with authentic standards of the oxidized linoleate moiety following its transesterification from the parental ceramide. The major hydroxy derivative in EOS was identified as 9-HODE, almost exclusively of the 9*R* chirality (Fig. 3*B*). The main keto derivative was 9-KODE (supplemental Fig. S2*B*). Transesterification of EpOH-EOS released one main epoxyalcohol, identified by normal phase HPLC, chiral HPLC, and GC-MS as 9*R*,10*R*-*trans*-epoxy-11*E*-13*R*-hydroxy-octadecenoate (Fig. 3*C* and supplemental Fig. S2*C*).

LOX Metabolites of Ceramides in Mouse Epidermis; Absence in 12R-LOX$^{-/-}$ Mice—The almost perfect match of *in vitro* and *in vivo* products made a compelling case for involvement of 12*R*-LOX and eLOX3 in oxygenation of the EOS ceramides in mammalian epidermis. This connection was further examined by analysis of endogenous LOX metabolites in mouse epidermis, in which the overall hypothesis could be tested using 12*R*-LOX$^{-/-}$ mice. Indeed, LOX metabolites of EOS were detected in wild-type mouse epidermis: 9*R*-HODE-EOS, and EpOH-EOS were present, although in minor abundance, and absent in 12*R*-LOX$^{-/-}$ epidermis (supplemental Figs. S3 and S4, *A* and *G*). The main LOX product in the mouse epidermal ceramides is a distinctive derivative of EpOH-EOS identified as epoxy-keto-EOS (see below), detected both as the free lipid (Fig. 4*A*, indicated on the *red* 235-nm trace, and supplemental Fig. S4, *A* and *F*) and as reversibly bound lipid in extracts of the proteins (Fig. 4*B* and supplemental Figs. S4, *C* and *H*, and S5). The ratio of the free to the reversibly protein-bound epoxy-keto-EOS was 0.89 ± 0.06 (S.E., $n = 4$).

The UV spectrum of the epoxy-ketone-EOS (Fig. 4*B*, *inset*) is characteristic of a conjugated enone with allylic epoxide (32). Its structural identification entailed reduction with sodium borohydride, transesterification to the methyl ester, and HPLC-UV and GC-MS analysis of the resulting epoxyalcohol methyl esters in comparison with authentic standards (Fig. 4, *C*

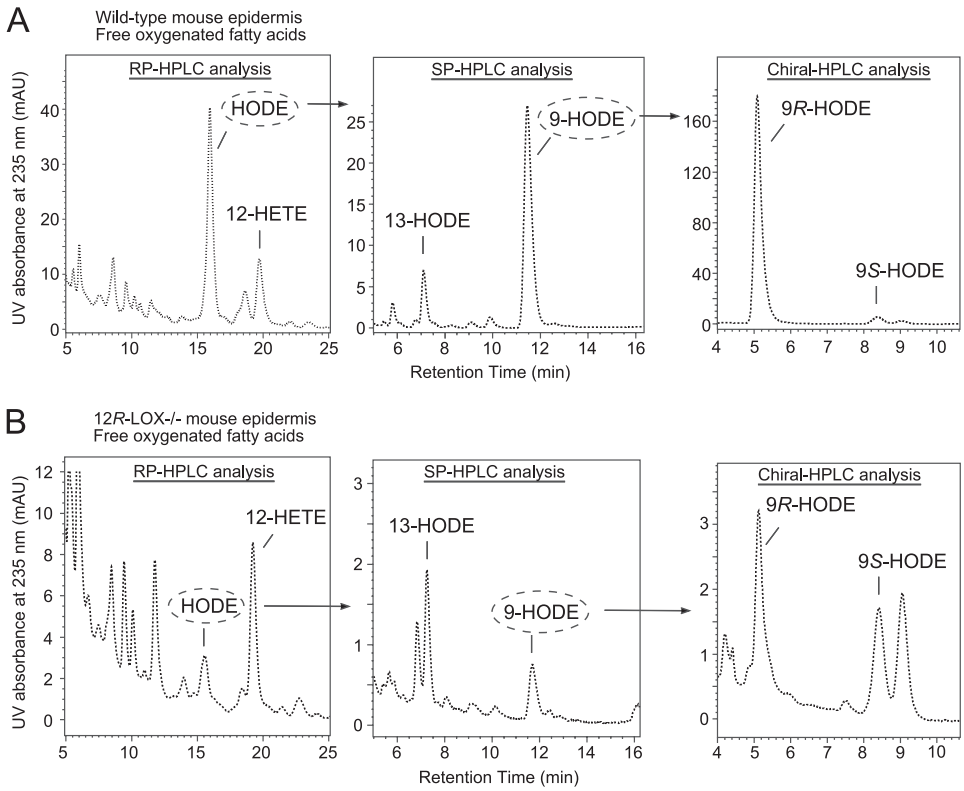

FIGURE 5. **Analysis of free oxygenated fatty acid metabolites from wild-type mouse epidermis (*A*) and from 12*R*-LOX$^{-/-}$ mouse epidermis (*B*).** *Left panels*, RP-HPLC analysis of free HODE and HETE. *Middle panels*, HODE was collected and further analyzed by normal phase HPLC. *Right panels*, 9-HODE was collected and further analyzed by chiral HPLC Free HODE and HETE eluted between 2 and 4 min in the normal phase HPLC analysis of total lipid extract as in Fig. 4*A*. Therefore, the fraction from 2 to 4 min was collected and then subjected to the RP-HPLC analysis shown here. Chiral HPLC analysis indicated that 12-HETE from both wild-type and 12*R*-LOX$^{-/-}$ epidermis was in *S* configuration (data not shown). Identical aliquots were injected in this wild type *versus* 12*R*-LOX$^{-/-}$ comparison. Shown are representative chromatograms from three independent experiments on three sets of wild-type and 12*R*-LOX$^{-/-}$ littermates. Note the 4- or 10-fold more sensitive *y* axis absorbance scale on the 12*R*-LOX$^{-/-}$ chromatograms.

and *D*). This main oxidized ceramide in mouse epidermis was thus identified as the purely chiral 9*R*,10*R*-*trans*-epoxy-11*E*-13-keto-octadecenoate-EOS (Fig. 4*D*). We have observed such epoxy-ketone derivatives as minor products in reactions of eLOX3 with fatty acid hydroperoxides (33), although its prominence in mouse epidermis suggests that a dehydrogenase may be involved in biosynthesis from its epoxyalcohol precursor.

The surprising finding of reversible binding of the epoxy-ketone to proteins was made during our procedures to exhaustively extract the free lipids (supplemental Fig. S5). Following four or five cycles of sonication and extraction with chloroform/methanol (1:1 or 2:1) for 1–2 h at 0 °C, HPLC analysis indicated no further detectable free lipid in the extracts. However, upon a further soak of the protein pellet in chloroform/methanol (1:1) at room temperature overnight, two classes of lipids were recovered: an early eluting epoxy-keto-ω-hydroxy-VLFA (Fig. 4*B* and supplemental Fig. S4, *D* and *I*) and epoxy-keto-EOS identical to that in the free ceramides (except that its VLFA component was mainly the longer C34:1 species, Fig. 4*B* and supplemental Fig. S4, *C* and *H*). To completely extract this pool of lipids, six or seven cycles of such prolonged incubations at room temperature were required. Like the other LOX metabolites, these products were completely absent in 12*R*-LOX$^{-/-}$ epidermis (Fig. 4*B*, *lower panel*).

We note that in the 12*R*-LOX$^{-/-}$ mouse epidermis, unmetabolized EOS is present at over twice the level of wild type (2.5 ± 0.2-fold, mean ± S.E., $n = 5$; Fig. 4*A*), a selective accumulation pointing to EOS as the LOX substrate. In essential fatty acid deficiency, a selective accumulation of oleate-substituted EOS is seen (17), which in light of our results is understandable because oleate is not a LOX substrate, and therefore its further metabolism is precluded. We also examined Glc-EOS, the precursor of EOS (34), and found no oxygenated metabolites in either pig or mouse epidermis, further suggesting that the LOX metabolism occurs during or after the transformation of Glc-EOS to EOS.

Identification of Free 9R-HODE in Mouse Epidermis—These results confirm the role of 12*R*-LOX and eLOX3 in production of the oxidized ceramides in the epidermis. Furthermore, an additional LOX product in wild-type epidermis was identified as free 9*R*-HODE, and this was also absent in the 12*R*-LOX$^{-/-}$ mice (Fig. 5). Because mouse 12*R*-LOX is inactive toward free linoleic acid (35, 36), the observed occurrence of free 9*R*-HODE points to its origin via hydrolysis of an esterified precursor, probably 9*R*-HODE-EOS. As proposed in our hypothesis, such a hydrolytic event following LOX metabolism is a crucial step in epidermal barrier formation.

Ester-linked Protein-bound Lipids in Mouse Epidermis—Central to our hypothesis is that the ester-linked protein-bound OS ceramides and ω-hydroxy-VLFA, the main components of the CLE, should be reduced or absent in 12*R*-LOX$^{-/-}$ mice. Although this has been suggested by prior TLC analysis

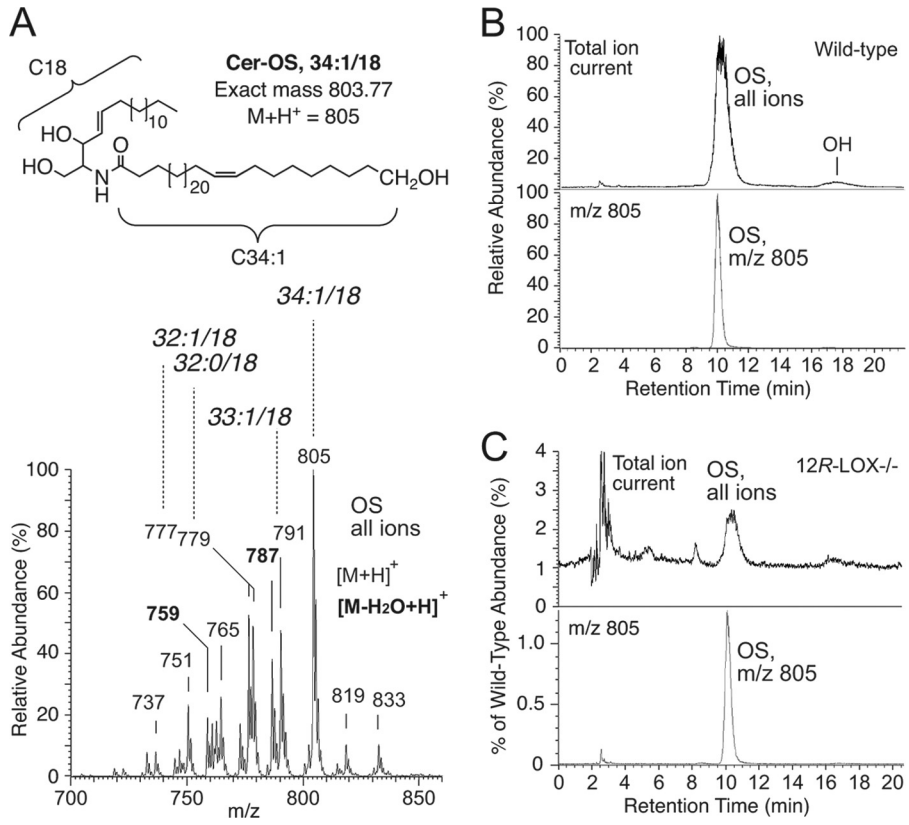

FIGURE 6. **Covalently bound ω-hydroxyceramides in mouse epidermis.** *A*, *top panel*, the structure of the most prominent OS species (M + 1 ion at *m/z* 805) released by mild alkaline hydrolysis from the proteins of wild-type epidermis. *Bottom panel*, APCI-MS of the mixture of all OS species. *B*, *top panel*, normal phase HPLC-APCI-MS analysis of bound ceramides from wild-type epidermis reveals a main peak of OS (ω-hydroxysphingosine) and minor OH (ω-hydroxy-hydroxysphingosine). *Bottom panel*, the profile of the OS species at *m/z* 805. *C*, the corresponding analysis of bound ceramides from 12*R*-LOX$^{-/-}$ epidermis. The height of the OS peak compared with wild type was 1.3% in this experiment and in four independent experiments averaged 0.8 ± 0.3% (S.E.).

(14), definitive evidence is lacking because the multiple spots on TLC were not characterized. Here we used LC-MS to analyze and compare the levels of the ester-linked protein-bound lipids in wild-type and 12*R*-LOX$^{-/-}$ mouse epidermis. The ester-linked lipids were obtained by mild-alkaline hydrolysis of the protein pellet after prior extensive extraction to remove any free or reversibly bound lipids. Using normal phase HPLC-APCI-MS and reversed phase HPLC-electrospray ionization-MS analyses, respectively, we identified OS and ω-hydroxy VLFA as the major covalently bound lipids in wild-type mouse epidermis (Fig. 6, *A* and *B*, and supplemental Fig. S6*A*). Similar to the reversibly bound lipids (supplemental Fig. S5), the composition of the VLFA in these irreversibly ester-linked lipids is different from that of free EOS ceramides, the most abundant being 34:1 (*m/z* 805, Fig. 6*A* and supplemental Fig. S6*C*). In sharp contrast to wild-type epidermis, the level of covalently bound OS in 12*R*-LOX$^{-/-}$ mice was only ~1% of the wild-type level (0.8 ± 0.3%, mean ± S.E., $n = 4$) (Fig. 6*C*). Similarly, covalently bound ω-hydroxy VLFA was 100-fold lower in 12*R*-LOX$^{-/-}$ mouse epidermis (0.9 ± 0.4% of wild type, mean ± S.E., $n = 3$) (supplemental Fig. S6*B*).

CLE Structure in Wild-type and 12R-LOX$^{-/-}$ Epidermis—Because the covalently bound ω-hydroxy derivatives are main components of the monolayer of lipids comprising the CLE, we next used electron microscopy to examine this structure in 12*R*-LOX$^{-/-}$ in comparison with wild-type epidermis. Consistent with the biochemical results, EM analysis revealed that

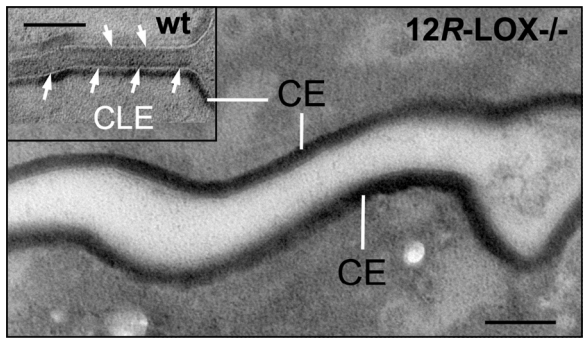

FIGURE 7. **12*R*-LOX$^{-/-}$ corneocytes lack visible CLE.** Although corneocytes from 12*R*-LOX$^{-/-}$ mice display normal CE, they lack externally apposed corneocyte lipid envelopes. The *inset* shows typical CLEs surrounding corneocytes in a wild-type (*wt*) littermate. *Scale bar*, 100 nm.

the CLE was virtually absent in 12*R*-LOX$^{-/-}$ mice (Fig. 7). These results prove unambiguously that 12*R*-LOX and eLOX3 are indispensably involved in the metabolic pathway of EOS that leads to the formation of covalently bound ω-hydroxyceramides and ω-hydroxy VLFA and the construction of a key component of the epidermal water barrier, the CLE.

DISCUSSION

Our study uncovers a novel biochemical pathway whereby 12*R*-LOX and eLOX3 mediate the long known and not well understood effect of EFA in skin barrier formation. In this pathway, 12*R*-LOX oxygenates the linoleate-containing EOS cera-

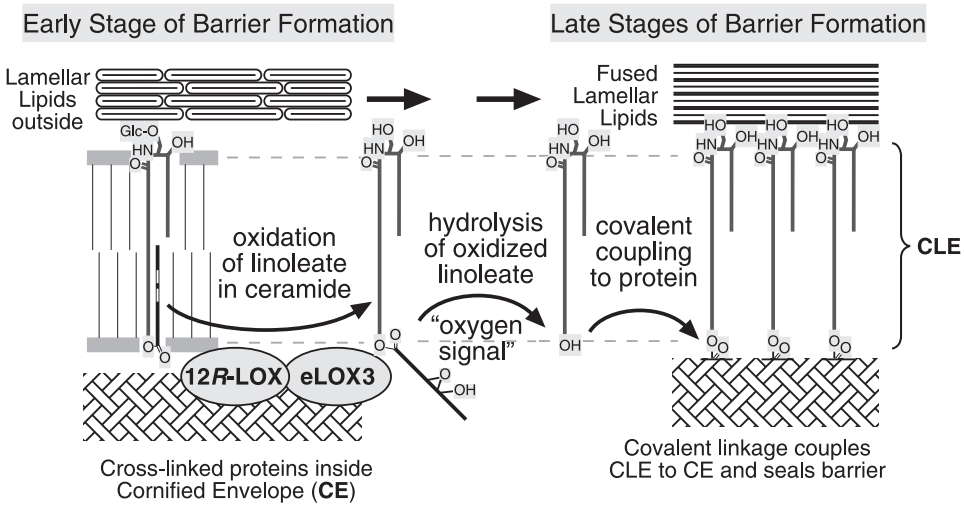

FIGURE 8. **Proposed model linking ceramides, EFA, and LOX in skin barrier formation.** Early events (not illustrated) involve fusion of lipid-containing lamellar granules with the corneocyte plasma membrane, extruding the lipid lamellar discs extracellularly and combining the granule limiting membrane (comprised of Glc-EOS) with the cell plasma membrane, initiating formation of the CLE (shown greatly expanded). Progression toward the mature barrier entails LOX-catalyzed oxygenation of the linoleate. The resultant "oxygen signal" permits esterase-catalyzed hydrolysis of the oxidized linoleate, freeing the ceramide ω-hydroxyl for transglutaminase-catalyzed covalent coupling of the lipids to the cross-linked proteins of the CE, thus forming the CLE and helping to seal the barrier. Lipoxygenase-catalyzed oxygenation of Glc-EOS may be initiated earlier in the process than illustrated here.

mides to give the 9*R*-hydroperoxide derivative, and eLOX3 in turn converts the 12*R*-LOX product to the specific 9*R*,10*R*-epoxy-13*R*-hydroxy-epoxyalcohol derivative. Furthermore, based on our biochemical and EM evidence that the CLE is missing in 12*R*-LOX$^{-/-}$ mice in correlation with a complete absence of LOX metabolites, we deduce that this LOX-catalyzed oxygenation is required to facilitate hydrolysis of the (oxidized) linoleate moiety and leave free the ω-hydroxyl on the ceramides for coupling to the cross-linked proteins of the CE (Fig. 8). This covalent coupling is an important step in sealing the water barrier (5, 37). If EFA are deficient, there is no LOX substrate available, and thus the fatty acid cannot be cleaved. Absence of one or the other of the LOX enzymes has a similar effect. Thus in both cases, the CLE is either missing or defective, leading to a skin barrier defect.

Our model linking EFA with the action of 12*R*-LOX and eLOX3 also provides a simple explanation for the findings of Houtsmuller and van der Beek (2) on the structural characteristics of EFA: for a fatty acid (natural or synthetic) to be able to cure the effects of EFA deficiency in the skin, it has to have at least two *cis* double bonds in the arrangement of bond-CH_2-bond and placed near the ω6 position from the end of the carbon chain (2), which fits perfectly with the structural requirement of LOX substrates. Thus, although other fatty acids such as 9-*trans*,12-*cis*-18:2ω6 or 9-*trans*,12-*cis*-18:2ω6 (which differ from linoleic acid only in the configuration of one double bond) will be incorporated into the EOS ceramides if topically applied to essential fatty acid-deficient skin (34), they invariably fail to cure the skin defects, according to our model because they are not LOX substrates. This line of thinking is not mutually exclusive with evidence that the special physical properties brought by linoleate itself in acylceramides contribute to another facet of epidermal barrier function, the proper phase behavior and structural organization of the intercellular lipid lamellae (38, 39).

In further support of our hypothesis, many papers over the years indicate that oxidized polyunsaturated fatty acid esters are more susceptible to hydrolysis from membrane lipids, and indeed nowadays it is generally accepted that oxidation disrupts membranes and provokes clearance of oxidized lipids (40–43). In our model, there is also the possibility that the specific oxygenation pattern brought by 12*R*-LOX and eLOX3 is stringently required by the downstream esterase for hydrolysis to occur.

It is worth mentioning at this point that EOS-related ceramides were proposed to be LOX substrates in the mid-1980s (34), at a time when this class of ceramides was newly discovered (44) and over 10 years before the discovery of 12*R*-LOX and eLOX3 (45, 46). When Nugteren *et al.* (34) applied [1-^{14}C]linoleic acid to the skin of EFA-deficient rats, 2 or 3 days later some of the radioactivity was recovered in a group of oxidized ceramides that were suggested to be LOX metabolites. Because of technical limitations at the time, these putative LOX metabolites were not structurally defined. Our present study demonstrates that the oxygenated metabolites of EOS found *in vivo* exhibit the same remarkably high regio- and stereospecificity as the LOX products *in vitro*, thus definitively resolving the arguments over whether the oxygenated metabolites were truly of enzymatic origin (47). Moreover, we have advanced a further step in rationalizing the functions these LOX metabolites may serve in the skin, *i.e.* to help build the CLE.

It was once assumed that arachidonic acid is the natural substrate of the putative 12*R*-LOX-eLOX3 pathway in the epidermis, being converted via 12*R*-HPETE to 8*R*-hydroxy-11*R*,12*R*-epoxyeicosa-5*Z*,9*E*,14*Z*-trienoic acid (16). A major problem with this assumption was that arachidonic acid is not a substrate of mouse 12*R*-LOX (35). Instead, the enzyme prefers to use fatty acid esters such as methyl arachidonate as substrate. This no longer presents as a problem, because we now suggest in this study that arachidonic acid oxygenation by 12*R*-LOX

and eLOX3 is of little relevance to the physiology of skin barrier formation. Nonetheless, the 12*R*-LOX products of arachidonic acid do occur in the inflammatory skin disease of psoriasis (48, 49) and may have a separate role in that condition.

In mouse epidermis, the EpOH-EOS product of eLOX3 was detected only as a minor metabolite, and the major metabolite was identified as 9*R*,10*R*-epoxy-13-keto-EOS. Such epoxy-ketone compounds are often formed as byproducts in the reactions of eLOX3 with fatty acid hydroperoxides (33). Because the detected LOX metabolites *in vivo* are likely to be "leftovers" from the downstream hydrolysis, one interpretation is that the epoxyalcohol derivative is preferentially hydrolyzed, whereas the byproducts are hydrolyzed to a lesser extent and thus accumulate. An alternative is an enzymatic step catalyzing the alcohol-to-ketone oxidation. Intriguingly approximately half of the epoxy-ketone-EOS in mouse epidermis, together with epoxy-ketone-acyl acids, is directly coupled to proteins through a reversible linkage. Most likely, the chemistry involves Michael addition of the α,β-unsaturated ketone to His on proteins (32). Notably, the CE protein involucrin is enriched in His (50). These potential non-ester-bound species cannot be distinguished from the ester-bound ω-hydroxyceramides using mild alkaline hydrolysis, because free ω-hydroxyceramides will also be recovered, whereas the oxidized linoleate will remain attached to proteins. Binding via the α,β-unsaturated ketone moiety could help juxtapose the EOS derivatives on the CE proteins, prior to the more permanent covalent linkage.

Our findings delineate the events in construction of the CLE and link EFA with LOX metabolism, an understanding with potential therapeutic implications related to treatments of the ichthyoses. Patients with inactivating mutations in ALOX12B or ALOXE3 lack the ability to oxidize the ceramides and cleave the linoleate moiety, and potentially this defect could be bypassed by topical application of LOX metabolites or free ω-hydroxyceramides. Understanding this pathway could also be beneficial in the treatment of patients with other forms of ichthyosis.

Acknowledgments—We thank Drs. David Hachey and Wade Calcutt for help with LC-MS, Jonas Perez and Dr. David Wright for help with the CD spectroscopy, Melanie Hupe for preparing the EM figure, and Drs. Ronald B. Emeson and Xiangli Yang for providing normal mouse tissues.

REFERENCES

1. Burr, G. O., and Burr, M. M. (1929) *J. Biol. Chem.* **82,** 345–367
2. Houtsmuller, U. M., and van der Beek, A. (1981) *Prog. Lipid Res.* **20,** 219–224
3. Akiyama, M., and Shimizu, H. (2008) *Exp. Dermatol.* **17,** 373–382
4. Fischer, J. (2009) *J. Invest. Dermatol.* **129,** 1319–1321
5. Uchida, Y., and Holleran, W. M. (2008) *J. Dermatol. Sci.* **51,** 77–87
6. Wertz, P. W., and Downing, D. T. (1987) *Biochim. Biophys. Acta* **917,** 108–111
7. Hedberg, C. L., Wertz, P. W., and Downing, D. T. (1988) *J. Invest. Dermatol.* **91,** 169–174
8. Doering, T., Brade, H., and Sandhoff, K. (2002) *J. Lipid Res.* **43,** 1727–1733
9. Nemes, Z., Marekov, L. N., Fésüs, L., and Steinert, P. M. (1999) *Proc. Natl. Acad. Sci. U.S.A.* **96,** 8402–8407
10. Swartzendruber, D. C., Wertz, P. W., Madison, K. C., and Downing, D. T. (1987) *J. Invest. Dermatol.* **88,** 709–713
11. Elias, P. M. (2005) *J. Invest. Dermatol.* **125,** 183–200
12. Jobard, F., Lefèvre, C., Karaduman, A., Blanchet-Bardon, C., Emre, S., Weissenbach, J., Özqüc, M., Lathrop, M., Prud'homme, J. F., and Fischer, J. (2002) *Hum. Mol. Genet.* **11,** 107–113
13. Moran, J. L., Qiu, H., Turbe-Doan, A., Yun, Y., Boeglin, W. E., Brash, A. R., and Beier, D. R. (2007) *J. Invest. Dermatol.* **127,** 1893–1897
14. Epp, N., Fürstenberger, G., Müller, K., de Juanes, S., Leitges, M., Hausser, I., Thieme, F., Liebisch, G., Schmitz, G., and Krieg, P. (2007) *J. Cell Biol.* **177,** 173–182
15. Krieg, P. (2010) *Exp. Dermatol.* **19,** 941–943
16. Yu, Z., Schneider, C., Boeglin, W. E., Marnett, L. J., and Brash, A. R. (2003) *Proc. Natl. Acad. Sci. U.S.A.* **100,** 9162–9167
17. Wertz, P. W., Cho, E. S., and Downing, D. T. (1983) *Biochim. Biophys. Acta* **753,** 350–355
18. Meguro, S., Arai, Y., Masukawa, Y., Uie, K., and Tokimitsu, I. (2000) *Arch. Dermatol. Res.* **292,** 463–468
19. Zheng, Y., Boeglin, W. E., Schneider, C., and Brash, A. R. (2008) *J. Biol. Chem.* **283,** 5138–5147
20. Coffa, G., and Brash, A. R. (2004) *Proc. Natl. Acad. Sci. U.S.A.* **101,** 15579–15584
21. Bligh, E. G., and Dyer, W. J. (1959) *Can. J. Biochem. Physiol.* **37,** 911–917
22. Farwanah, H., Wohlrab, J., Neubert, R. H., and Raith, K. (2005) *Anal. Bioanal. Chem.* **383,** 632–637
23. Butovich, I. A., and Reddy, C. C. (2001) *Biochim. Biophys. Acta* **1546,** 379–398
24. Zheng, Y., and Brash, A. R. (2010) *J. Biol. Chem.* **285,** 13427–13436
25. Galliard, T., and Phillips, D. R. (1971) *Biochem. J.* **124,** 431–438
26. Peers, K. E., and Coxon, D. T. (1983) *Chem. Phys. Lipids* **32,** 49–56
27. Chang, M. S., Boeglin, W. E., Guengerich, F. P., and Brash, A. R. (1996) *Biochemistry* **35,** 464–471
28. Schneider, C., Schreier, P., and Humpf, H. YU. (1997) *Chirality* **9,** 563–567
29. Behne, M., Uchida, Y., Seki, T., de Montellano, P. O., Elias, P. M., and Holleran, W. M. (2000) *J. Invest. Dermatol.* **114,** 185–192
30. Wertz, P. W., and Downing, D. T. (1983) *J. Lipid Res.* **24,** 753–758
31. Hamanaka, S., Asagami, C., Suzuki, M., Inagaki, F., and Suzuki, A. (1989) *J. Biochem.* **105,** 684–690
32. Lin, D., Zhang, J., and Sayre, L. M. (2007) *J. Org. Chem.* **72,** 9471–9480
33. Zheng, Y., and Brash, A. R. (2010) *J. Biol. Chem.* **285,** 39876–39887
34. Nugteren, D. H., Christ-Hazelhof, E., van der Beek, A., and Houtsmuller, U. M. (1985) *Biochim. Biophys. Acta* **834,** 429–436
35. Siebert, M., Krieg, P., Lehmann, W. D., Marks, F., and Fürstenberger, G. (2001) *Biochem. J.* **355,** 97–104
36. Meruvu, S., Walther, M., Ivanov, I., Hammarström, S., Fürstenberger, G., Krieg, P., Reddanna, P., and Kuhn, H. (2005) *J. Biol. Chem.* **280,** 36633–36641
37. Madison, K. C. (2003) *J. Invest. Dermatol.* **121,** 231–241
38. Bouwstra, J. A., Gooris, G. S., Dubbelaar, F. E., and Ponec, M. (2002) *J. Invest. Dermatol.* **118,** 606–617
39. Groen, D., Gooris, G. S., and Bouwstra, J. A. (2010) *Langmuir* **26,** 4168–4175
40. Sevanian, A., and Kim, E. (1985) *J. Free Radic. Biol. Med.* **1,** 263–271
41. Feussner, I., Wasternack, C., Kindl, H., and Kühn, H. (1995) *Proc. Natl. Acad. Sci. U.S.A.* **92,** 11849–11853
42. Belkner, J., Stender, H., Holzhütter, H. G., Holm, C., and Kühn, H. (2000) *Biochem. J.* **352,** 125–133
43. Stafforini, D. M., Sheller, J. R., Blackwell, T. S., Sapirstein, A., Yull, F. E., McIntyre, T. M., Bonventre, J. V., Prescott, S. M., and Roberts, L. J., 2nd. (2006) *J. Biol. Chem.* **281,** 4616–4623
44. Wertz, P. W., and Downing, D. T. (1982) *Science* **217,** 1261–1262
45. Boeglin, W. E., Kim, R. B., and Brash, A. R. (1998) *Proc. Natl. Acad. Sci. U.S.A.* **95,** 6744–6749
46. Kinzig, A., Heidt, M., Fürstenberger, G., Marks, F., and Krieg, P. (1999) *Genomics* **58,** 158–164
47. Wertz, P. W., and Downing, D. T. (1990) *J. Lipid Res.* **31,** 1839–1844
48. Brash, A. R., Yu, Z., Boeglin, W. E., and Schneider, C. (2007) *FEBS J.* **274,** 3494–3502
49. Woollard, P. M. (1986) *Biochem. Biophys. Res. Commun.* **136,** 169–176
50. Downing, D. T. (1992) *J. Lipid Res.* **33,** 301–313